2019 American Control Conference (ACC)
Philadelphia, PA, USA, July 10-12, 2019

A Regularized System Identification Approach to Subject-Specific Physiological Modeling with Limited Data*

Ali Tivay, Ghazal Arabi Darreh Dor, Ramin Bighamian, George C. Kramer, and Jin-Oh Hahn, *Senior Member, IEEE*

***Abstract*—This paper investigates a novel regularized system identification approach to physiological modeling using limited data. The proposed approach operates in two steps: 1) limited data from individual subjects are consolidated and leveraged to determine a population-average physiological model; then, 2) a subject-specific model for an individual subject is derived from a regularized system identification procedure whose objective is to reconcile the model's capability to predict individual-specific behavior and to retain typical population-representative trends. This is achieved by embedding a regularizing condition into the cost function for system identification that enforces parsimony in parametric deviation from the population-average model. A few unique advantages of the proposed approach are that 1) it offers superior predictive accuracy in both measured as well as unmeasured physiological system responses when compared to a standard system identification approach; and 2) it provides high-sensitivity parameters in the model associated with each individual subject, thus potentially eliminating the necessity for post-hoc parametric sensitivity analysis. Merits and limitations of the proposed regularized approach are illustrated with a real world case study on physiological modeling of hemodynamics in response to burn injury and resuscitation.**

I. Introduction

Development of a parsimonious and transparent model of a physiological system is an important pre-requisite toward disciplined closed-loop automation of therapy in critically ill patients. To be useful, such a physiological model must show the relevant macroscopic behavior of a patient's response to therapy using meaningful components and interactions. A grey-box modeling approach is often desirable in this regard as it provides opportunity for both robust estimation of model parameters from experimental data as well as transparency of model structure.

A unique, important challenge in modeling physiological systems lies in the variability of behavior between individual subjects. While an individualized model is desirable in order to capture subject-specific behavior, available data from real clinical scenarios are often sparse, limited and non-standardized. Using such data for system identification often results in an over-fitted model in which internal component interactions are not predicted accurately. Having limited data also directly affects the sensitivity of model output error to changes in model parameters. This results in the presence of insensitive parameters that do not affect the output prediction error significantly, or redundant subsets of parameters that exhibit the same effect on the measured output.

A prevalent class of approaches to partially address this problem are based on the concept of parametric sensitivity analysis: variance-based approaches such as Sobol [1] and Monte-Carlo [2] techniques give useful information about the effect of each parameter and also parametric combinations on the model output, while profile likelihood [3] approaches give valuable insight into redundancies among parameters and opportunities for potentially useful extra measurements. Conducting sensitivity analysis, however, does not always give a clear pathway toward preventing the negative effects of limited data on the model's predictive capability. One effective solution to this problem would be to fix insensitive parameters to nominal values [4], [5]. Another interesting solution is to simplify the model toward a more lumped macroscopic structure [6], [7]. Alternatively, one can prevent overfitting to limited data by adding acceleration terms to the error minimization algorithm [8]. Parameter regularization [9], [10] and assumption of Bayesian priors [11] are also effective tools widely used in data-based black-box modeling and machine learning applications to prevent an extremely complex or unidentifiable model structure.

The challenge in using most of the reviewed methods for therapy-oriented modeling of physiological systems is that both the quality (e.g., sampling frequency and measurement noise) and quantity (e.g., number of measured signals) of data drastically vary across subjects. In addition, each subject is an inherently unique entity with subject-specific characteristics. Because of this, identifiability of the model varies on a case by case basis, thus preventing a unified approach to tackle the system identification problem across all subjects. Therefore, an individualized system identification approach that takes into consideration the variability in both data and subjects is desirable.

In our initial attempt to address this issue, we investigate a regularized system identification approach to physiological modeling with limited data. The proposed approach operates in two steps: by first deriving a population-average model from data consolidated across all subjects, then by deriving a subject-specific model associated with an individual from the limited subject-specific data. This is achieved by proposing a regularized system identification procedure, the goal of which is to reconcile the model's ability to predict subject-specific behavior and to retain typical population-based trends. This goal is achieved by embedding a regularizing condition into the cost function used in system identification that enforces parsimony in parametric deviation from the population-average model. Key unique advantages of the proposed approach are 1) its superior predictive accuracy relative to standard error-minimizing system identification by

*Research supported by National Science Foundation CAREER Award (Grant No. 1748762) and Arcos, Inc. (Contract No. 29882).

A. Tivay, G. Arabi Darreh Dor, and J.O. Hahn are with the Mechanical Engineering Department, University of Maryland, College Park, MD 20742 USA (phone: 301-405-7864; fax: 301-314-9477; e-mail: tivay@umd.edu).

R. Bighamian is with the Electrical Engineering Department, University of Southern California, Los Angeles, CA 90089 USA.

G. Kramer is with the Anesthesiology Department, University of Texas Medical Branch, Galveston, TX 77555 USA.

avoiding subject-specific overfitting and 2) its ability to determine high-sensitivity model parameters as part of the system identification procedure, thereby eliminating the need for separate post-hoc parametric sensitivity analysis. Merits and limitations of the proposed approach are illustrated with a clinically important case study on physiological modeling of hemodynamic responses to burn injury and resuscitation.

II. A Regularized System Identification Approach to Subject-Specific Physiological Modeling

A. Rationale

In contrast to conventional engineering and statistical applications, modeling of physiological systems based on an entire population sample does not always give sufficiently predictive models due to large inter-individual variability. However, there are general trends of behavior in measured data that hold in most subjects. On the other hand, subject-specific modeling using a parameterized grey-box model can be susceptible to overfitting due to the lack of sufficient information content in the data. Yet, it is still likely to better predict an individual subject's behavior if the identification problem is properly formulated. An ideal approach to follow in this situation would leverage both population-average and subject-specific trends to obtain a model for each individual.

B. Formulation of Regularized System Identification

The structure of the dynamic physiological model is defined for each individual i as follows:

$$\begin{aligned} \dot{x} &= f(x,u,p^{(i)},t) \\ y_j &= g_j(x,p^{(i)}) \end{aligned} \tag{1}$$

where the grey-box model structure f is assumed to be the same for all individuals, while each individual is characterized by an unknown vector of parameters $p^{(i)}$. Each of the outputs y_j correspond to a signal of interest measured at least in some subjects.

To consolidate a population-average model of the common behavior across all subjects, we define the following error measure:

$$\bar{f}(p) = \sum_{i=1}^{N}\sum_{j=1}^{M_i}\sum_{k=1}^{D_{ij}}\left(\frac{y_j^d(t_k) - y_j(p,t_k)}{\bar{y}_j}\right)^2 \tag{2}$$

where N is the number of subjects, M_i is the number of measured signals for subject i, D_{ij} shows the number of measurements for signal j taken from subject i, $y_j^d(t_k)$ denotes the value of measured signal j at time t_k, and $\bar{y}_j$ is the normalization factor for signal j.

The population-average model can be obtained from the following optimization problem:

$$\bar{p} = \arg\min_p \bar{f}(p) \tag{3}$$

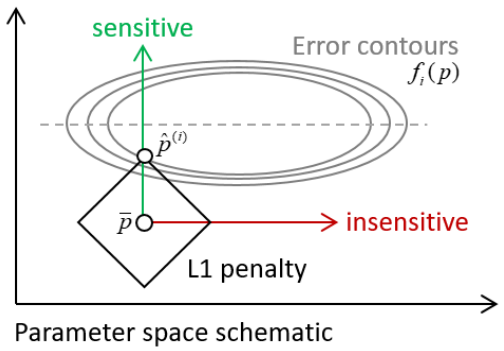

Figure 1. Schematic illustration of the penalized optimization problem for individual-specific systems identification

where the resulting minimizer $\bar{p}$ can be used with (1) to obtain a dynamic model that represents the common trends of average behavior across all subjects.

A standard least-squares error-minimization approach to deriving a subject-specific model for a new individual uses the following cost formulation:

$$f_i(p) = \sum_{j=1}^{M_i}\sum_{k=1}^{D_{ij}}\left(\frac{y_j^d(t_k) - y_j(p,t_k)}{\bar{y}_j}\right)^2 \tag{4}$$

from which a parameter vector $\hat{p}^{(i)}$ can be obtained for each new subject from the following minimization problem:

$$\hat{p}^{(i)} = \arg\min_p f_i(p) \tag{5}$$

This optimization problem, however, can be ill-posed as an inverse problem due to both the grey-box structure of the model and the limited nature of individual-specific data. When solving (5), there can be many vector parameters $\hat{p}^{(i)}$ that result in equivalently low values for the error measure (4), which often results in blow-ups in parameter values after optimization and deteriorated predictive value in the resulting model.

To counteract the effects of limited data, we propose to incorporate a regularizing term in the cost function (5) to substitute the measurements that are not available for new subjects:

$$\hat{p}^{(i)} = \arg\min_p f_i(p) + \Omega(p) \tag{6}$$

where $\Omega(p)$ incorporates information related to whether a parameter vector is a good choice for an individual. For the purpose of individual identification, we define the following candidate function:

$$\Omega(p) = \lambda\left\|p - \bar{p}\right\|_1 \tag{7}$$

where the norm $\|.\|_1$ denotes the absolute sum of vector elements. Fig. 1 visualizes the role of this penalty in a simple 2-parameter model identification scenario. It is visible from the error contours that the data do not contain discriminating information in the horizontal direction. As a result, the optimization in (5) can result in many equivalent answers

across the dashed line. The added penalty term (7) has sharp contour edges in the direction of each parameter, favoring solutions that only deviate in parameters having significant impact on the reduction of the output prediction error (which is the vertical direction in the case of Fig. 1). In the insensitive horizontal direction, the algorithm tends to fall back to the population-average value. In general, the penalty (7) tends to constrain deviations from the population-average model both in terms of distance and number of deviated parameters, unless such a deviation is absolutely needed to capture the unique behavior of the individual subject.

The potential advantages of this approach are two-fold: First, constraining parametric deviations reduces the risk of overfitting by minimizing the effective number of model parameters (i.e., model parameters that are individualized) for each individual. Second, analyzing the resulting model parameter deviations from population-average values can give insight into the important parameters in the model, thus potentially eliminating the need for post-hoc sensitivity analysis. In fact, parameters deviated from the population-average values tend to be the ones that 1) largely affect the system output, 2) represent useful information contained in the subject-specific data, and 3) tend to vary in different subjects. All three of these characteristics are indicative of parameters that are important to identify in a subject-specific setting.

III. Physiological Modeling of Hemodynamics in Response to Burn Injury and Resuscitation

A. Motivation

Fluid resuscitation is an integral part of critical care for burn injury patients, in which fluid infusion is administered to maintain a safe blood volume level within the patient's circulation [4], [12]. Reliable and transparent mathematical modeling of a patient's physiological responses to burn injury and fluid resuscitation is an important pre-requisite toward understanding and testing of resuscitation protocols as well as realizing closed-loop automation of burn resuscitation.

This application is a particularly interesting case study for the presented regularized identification method due to the limited and variable nature of its data as well as the existence of explicit inherent differences in individual subjects (e.g. different bodily characteristics for each individual as well as different impact of injury).

B. Mathematical Model of Hemodynamics in Response to Burn Injury and Resuscitation

In this section, we present a dynamic model structure to represent macroscopic components and interactions relevant to a patient's response to burn injury and resuscitation, which is an updated version of the models presented in the literature [4]. The model (shown in Fig. 2) consists of three main compartments in interaction, governed at the high level by the following differential equations:

$$\dot{V}_{ti} = J_{f,ti} - J_{l,ti} - J_{e,ti} \tag{8}$$

$$\dot{M}_{ti} = Q_{f,ti} - Q_{l,ti} \tag{9}$$

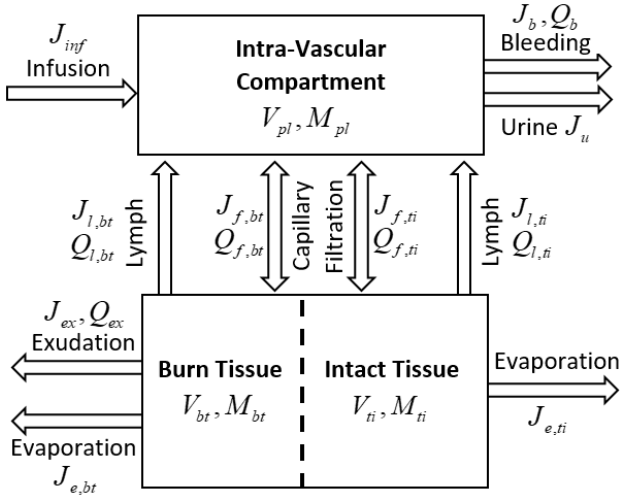

Figure 2. Schematic illustration of the multi-compartment fluid and protein kinetics model used for data-driven modeling of hemodynamic response to burn injury and resuscitation

$$\dot{V}_{bt} = J_{f,bt} - J_{l,bt} - J_{e,bt} - J_{ex} \tag{10}$$

$$\dot{M}_{bt} = Q_{f,bt} - Q_{l,bt} - Q_{ex} + Q_d \tag{11}$$

$$\dot{V}_{pl} = J_{\inf} - J_{f,ti} + J_{l,ti} - J_{f,bt} + J_{l,bt} - J_b - J_u \tag{12}$$

$$\dot{M}_{pl} = -Q_{f,ti} + Q_{l,ti} - Q_{f,bt} + Q_{l,bt} - Q_b \tag{13}$$

where the states denoted by V and M respectively represent fluid volume and protein mass inside each compartment, and subscripts "bt", "ti", and "pl" respectively denote burn-tissue interstitium, intact-tissue interstitium, and intra-vascular plasma compartments. The terms shown by J and Q respectively denote the rate of fluid flow and protein mass transfer between compartments as shown in Fig. 2.

The effective concentration of protein in each compartment is given by the following relations:

$$C_x = M_x / V_x \tag{14}$$

$$C_{x,av} = M_x / (V_x - V_{x,ex0}) \tag{15}$$

where $x \in \{ti, bt, pl\}$ denotes the compartment, C_x shows protein concentration, and $C_{x,av}$ shows protein concentration where some of the fluid volume $V_{x,ex0}$ is not participating in the calculation.

The presence of fluid and protein causes hydrostatic and oncotic pressures in each compartment:

$$P_{pl} = K_{ppl}(V_{pl} - V_{pl0}) + P_{pl0} \tag{16}$$

$$P_x = f_P(V_x) \tag{17}$$

$$\Pi_{pl} = K_\Pi C_{pl} \tag{18}$$

$$\Pi_x = K_\Pi C_{x,av} \tag{19}$$

where the vascular compartment pressure P_{pl} has a linear relationship with volume changes from the baseline V_{pl0} through K_{ppl}, and P_{pl0} denotes pressure at baseline volume. P_x shows pressure in either of the interstitial compartments

denoted by $x \in \{ti, bt\}$ calculated from an empirically-derived relationship $f_P(V_x)$ with compartmental fluid volume. The oncotic pressures Π_{pl}, Π_x in each compartment have a linear relationship with the effective protein concentration in that compartment, the slope of which is determined by constant K_Π.

Capillary filtration is one of the main ways of fluid and protein exchange between the vascular and tissue compartments. The rate of fluid exchange is given by the Starling equation as follows:

$$J_{f,x} = K_{f,x}\left(P_{pl} - P_x - \sigma_x(\Pi_{pl} - \Pi_x)\right) \tag{20}$$

where $K_{f,x}$ and σ_x are filtration and reflection coefficients respectively and $x \in \{ti, bt\}$ denotes the compartments. This equation determines the rate of fluid shift to tissue based on hydrostatic and oncotic pressure differences.

The rate of protein exchange is given by the coupled convective and diffusive transport relations of protein and fluid across the micro-vascular exchange system, which can be written as follows:

$$Q_{f,x} = J_{f,x}(1-\sigma_x)\left(\frac{C_{pl} - C_{x,av}\exp\left(-\frac{(1-\sigma_x)J_{f,x}}{A_x}\right)}{1-\exp\left(-\frac{(1-\sigma_x)J_{f,x}}{A_x}\right)}\right) \tag{21}$$

where A_x denotes the permeability-surface-area product for each of the compartments in exchange with the intra-vascular compartment.

Both $K_{f,x}$ and A_x in (20) and (21) are quantities that are affected by the amount of volume present in the intra-vascular compartment, as a higher volume tends to increase the effective surface area at the barrier between vascular and tissue spaces. The dependence on volume is formulated as follows:

$$R_{Vpl} = \frac{(V_{pl}/V_{pl0}) - V_{base}}{1 - V_{base}} \tag{22}$$

$$K_{f,x} = K_{f,nl} R_{Vpl} \tag{23}$$

$$A_x = A_{nl} R_{Vpl} \tag{24}$$

where R_{Vpl} is a ratio that models dependence of filtration surface area on plasma volume, V_{base} is the plasma volume at which there is zero fluid transport into the tissues, and $K_{f,nl}$, A_{nl} are filtration and permeability coefficients at normal plasma volume $V_{pl,0}$.

Lymphatic flow is another important mechanism of fluid and protein transport from both tissue compartments back into the intra-vascular space. The changes in the flow of lymph is mainly dependent on pressures inside the tissue. The equations for lymphatic flow are the following:

$$J_{l,x} = \begin{cases} J_{l,nl,x} + S_x(P_x - P_{x,nl}) & P_{x,nl} \le P_x \\ J_{l,nl,x}\left(\frac{P_x - P_{x,ex}}{P_{x,nl} - P_{x,ex}}\right) & P_{x,ex} \le P_x < P_{x,nl} \\ 0 & P_x < P_{x,ex} \end{cases} \tag{25}$$

where the pressure $P_{x,nl} = f_P(V_{x,nl})$ is associated with normal tissue pressure at a normal volume $V_{x,nl}$, and $P_{x,ex} = f_P(V_{x,ex})$ is the pressure at which lymphatic flow vanishes, evaluated at the minimum tissue volume $V_{x,ex}$. The subscript $x \in \{ti, bt\}$ denotes values for burn and intact tissue compartments. The term $J_{l,nl,x}$ represents the normal lymphatic flow rate for each compartment, and the constant S_x denotes the sensitivity of lymphatic flow to tissue pressure.

The transported protein along with the lymphatic flow from each of the tissue compartments can be calculated as:

$$Q_{l,x} = C_x J_{l,x} \tag{26}$$

where $x \in \{ti, bt\}$ represents each compartment.

The effects of burn injury are modeled as perturbations to pressure, content and filtration characteristics of the burn tissue, which can be summarized as follows:

$$K^*_{f,bt} = K_{f,nl} R_{Vpl}\left(1 + G_{Kf,bt}e^{-rt}\right) \tag{27}$$

$$A^*_{bt} = A_{nl} R_{Vpl}\left(1 + G_{A,bt}e^{-rt}\right) \tag{28}$$

$$\sigma^*_{bt} = \sigma_{nl}\left(1 - G_{\sigma,bt}e^{-rt}\right) \tag{29}$$

$$P^*_{bt} = f_P(V_{bt}) - G_{p,bt}e^{-ht} \tag{30}$$

$$Q_d = G_{den}e^{-ht} \tag{31}$$

where burn injury effects consist of time-variant perturbations to normal parameters with magnitudes denoted by $G_{Kf,bt}$, $G_{A,bt}$, and $G_{\sigma,bt}$. The constant r represents the rate of recovery post-burn, which causes the perturbed parameters to gradually return to their original value. In addition, P^*_{bt} is a perturbed version of tissue pressure that causes a suction effect into the burn tissue immediately after injury, with magnitude $G_{p,bt}$. Furthermore, Q_d represents the collagen denaturation phenomenon as a consequence of burn, which affects the effective protein content of the burn tissue. The exponent h is chosen as a relatively large number to achieve an impulse-like effect immediately after injury.

C. Experimental Burn Injury and Resuscitation Data

The experimental data used for this study come from eight sheep subjects exposed to burn injury and subsequent resuscitation with the Lactated Ringer's infusion. The study procedure was approved by the Institutional Animal Care and Use Committee (IACUC). Readers can refer to [12] for details about the study protocol. A summary of available measurements for the eight subjects is shown in Table I. The measurements have a variable time-resolution with at least hourly measurements in the first 12 hours post-burn and less frequent data points up to 72 hours post-burn.

TABLE I. SUMMARY OF AVAILABLE SUBJECT DATA

S.	Measurement							
	J_i	J_u	V_{pl}	C_{pl}	$J_{l,bt}$	$J_{l,ti}$	C_{bt}	C_{ti}
1	X	X	X	X		X		X
2	X	X	X	X		X		X
3	X	X	X	X		X		X
4	X	X	X		X	X		
5	X	X	X		X	X		
6	X	X	X		X	X		
7	X	X	X	X	X	X	X	X
8	X	X	X	X	X	X	X	X

D. Subject-Specific Burn Injury and Resuscitation Modeling via Regularized System Identification

To examine the merits and limitations of the proposed regularized identification method, we consider the scenario where only limited plasma volume data (V_{pl}) is available for each new subject, and the goal is to extract useful subject-specific information from this limited signal without deteriorating the integrity of the model.

For the purpose of evaluation, first, we exclude a subject s_i from the data shown in Table I. Then, a population-average model $\bar{p}$ is formed from incorporating the remaining data into the optimization procedure (3). Then, an individualized model is found for the excluded subject s_i by presenting its limited V_{pl} data along with $\bar{p}$ to the procedure in (6). The identified parameters are the following 13 parameters in the model:

$$p = [\ \sigma_{nl} \quad K_{f,nl} \quad J_{l,nl} \quad S_{nl} \quad A_{nl} \quad P_{pl0} \quad \dots \quad r \quad K_{ppl} \quad G_{den} \quad G_{p,bt} \quad G_{A,bt} \quad G_{Kf,bt} \quad G_{\sigma,bt}\ ] \quad (32)$$

We define the following error measures for each studied subject:

$$MSE = E(V_{pl}) \quad (33)$$

$$OMSE = E(C_{pl}, J_{l,bt}, J_{l,ti}, C_{ti}, C_{bt}) \quad (34)$$

where MSE represents the mean-squared error related to the limited signals presented to the individualized identification algorithm, while OMSE represents error for the other signals not presented to the algorithm. The operator $E(.)$ normalizes and calculates the error for the given signals. A subject-specific identification procedure that is immune to limited data would identify a model for a subject, which can provide reasonable predictions of signals not presented in the modeling stage (i.e., yield lower values for OMSE).

IV. RESULTS AND DISCUSSION

Fig. 3 presents a comparison of model predictions for regularized versus un-regularized (error-minimizing) system identification methods based on limited plasma volume data. System identification without regularization results in the best fit for plasma volume (MSE) but it severely deteriorates predictions for internal signals (OMSE) such as lymphatic flow, which indicates severe overfitting to limited data. The proposed regularized identification method still moves toward improved MSE with the advantage of maintaining sensible predictions for internal signals.

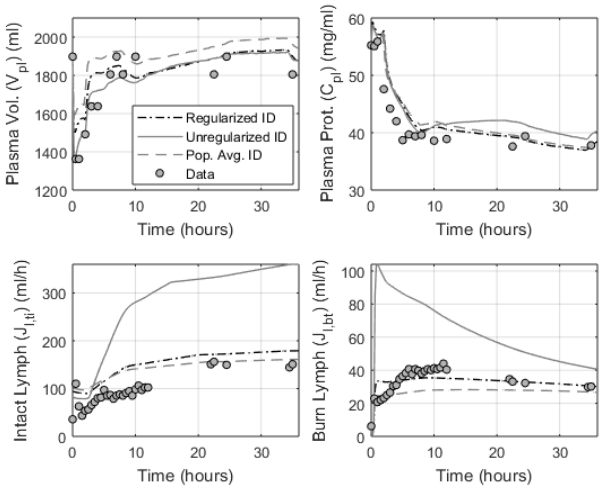

Figure 3. Comparison of regularized and un-regularized subject-specific identification based on limited plasma volume data (Subject 7).

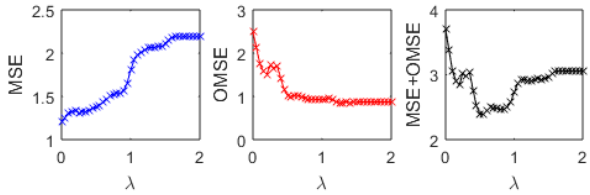

Figure 4. Comparison of MSE, OMSE and their sum for different penalty weights, averaged over all subjects

Fig. 4 shows MSE and OMSE with respect to penalty weights, averaged over all subjects. The errors at $\lambda = 0$ correspond to un-regularized identification, while the errors at $\lambda = 2$ correspond to the population-average model. For a λ between these two extremes (e.g., $\lambda = 0.6$) the value of MSE is close to the un-regularized case while OMSE is significantly reduced. These results indicate that the proposed identification procedure can make use of limited data without compromised predictions for internal signals.

Table II compares MSE and OMSE values in each subject for regularized versus un-regularized identification methods. As expected, MSE values are smallest in standard systems identification. However, this can be attributed to overfitting, as suggested by large OMSE values. The regularized approach results in higher levels of MSE than its un-regularized counterpart. However, most OMSE values are significantly improved, which indicates the robustness of the model against limited data.

Fig. 5 shows parametric deviations from the population-average model for all individual models obtained from the regularized approach. In all subjects, most parameters tended to adhere to their population-average values. As expected, only a few parameters of significance deviated from the population average values in each subject, which happens according to their sensitivity and the information present in the given data.

TABLE II. COMPARISON OF MSE AND OMSE FOR FREE VS REGULARIZED SUBJECT-SPECIFIC SYSTEM IDENTIFICATION

Subj.	Un-regularized ($\lambda = 0$)		Regularized ($\lambda = 0.6$)	
	MSE	OMSE	MSE	OMSE
1	1.12	0.53	1.14	0.47
2	0.90	0.48	0.90	0.47
3	1.58	1.88	1.64	2.30
4	1.78	1.17	1.88	1.00
5	1.72	5.63	2.52	1.87
6	1.25	0.85	1.31	0.77
7	0.55	3.46	0.97	0.87
8	0.81	5.90	0.92	0.79
mean	**1.21**	**2.48**	**1.41**	**1.06**

Fig. 6 shows the percentage of subjects for which each parameter deviated from its population-average value. For limited plasma volume data, the reflection coefficient σ_{nl} was the parameter that deviated the most across subjects. Due to the sparsity-promoting nature of the identification method, a deviation happens when a parameter is sensitive with respect to the studied output and the information in measurements warrants such a deviation. Physiologically, the importance of the reflection coefficient is well-known in determining the amount of fluid and protein shift out of plasma volume. For the studied case, the deviation-based analysis shown in Fig. 5 and Fig. 6 gives insight into both the sensitivity of each parameter and the parameter-relevant information present in output measurements.

V. CONCLUSION

In this paper, we proposed and investigated a regularized system identification approach to the physiological modeling problem with limited data. A generalizable framework was presented, and an embodiment of the approach was assessed using a clinically significant case study on the physiological modeling of hemodynamics in response to burn injury and resuscitation. The results strongly suggested the validity and potential of the regularized system identification approach: it may outperform both population-average and un-regularized error-minimization-based modeling approaches in terms of predictive accuracy, and it may also provide high-sensitivity model parameters as part of the system identification procedure. Future effort should be invested to more in-depth development of the proposed approach, investigation of a wide range of embodiment alternatives, and application of the approach to wide-ranging case studies to confirm the generalizability of the findings derived from this pilot work.

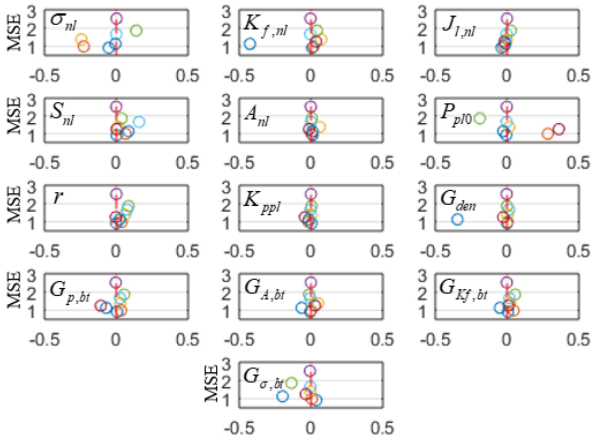

Figure 5. Parametric deviation ($p^{(i)} - \bar{p}$) results for the regularized identification approach (Horizontal axis: normalized deviation amount, colored dots: subject-specific deviations).

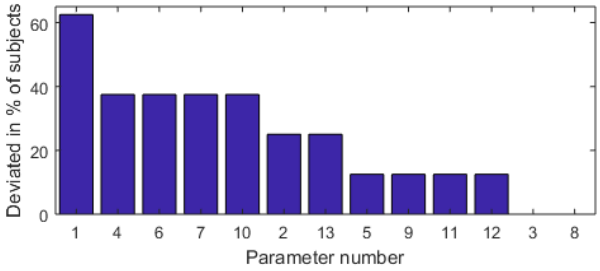

Figure 6. Sorted parameters in terms of the number of subjects for which they deviated from the population-average value

REFERENCES

[1] A. Saltelli, P. Annoni, I. Azzini, F. Campolongo, M. Ratto, and S. Tarantola, "Variance based sensitivity analysis of model output. Design and estimator for the total sensitivity index," *Comput. Phys. Commun.*, vol. 181, no. 2, pp. 259–270, Feb. 2010.

[2] I. . Sobol′, "Global sensitivity indices for nonlinear mathematical models and their Monte Carlo estimates," *Math. Comput. Simul.*, vol. 55, no. 1–3, pp. 271–280, Feb. 2001.

[3] A. Raue *et al.*, "Structural and practical identifiability analysis of partially observed dynamical models by exploiting the profile likelihood," *Bioinformatics*, vol. 25, no. 15, pp. 1923–1929, Aug. 2009.

[4] R. T. Ampratwum, B. D. Bowen, T. Lund, R. K. Reed, and J. L. Bert, "A model of fluid resuscitation following burn injury: formulation and parameter estimation," *Comput. Methods Programs Biomed.*, vol. 47, no. 1, pp. 1–19, Jun. 1995.

[5] X. Jin and J.-O. Hahn, "Semi-adaptive switching control for infusion of two interacting medications," *Biomed. Signal Process. Control*, vol. 43, pp. 183–195, May 2018.

[6] R. Bighamian, B. Parvinian, C. G. Scully, G. Kramer, and J.-O. Hahn, "Control-oriented physiological modeling of hemodynamic responses to blood volume perturbation.," *Control Eng. Pract.*, vol. 73, no. April 2018, pp. 149–160, Apr. 2018.

[7] M. K. Transtrum and P. Qiu, "Bridging Mechanistic and Phenomenological Models of Complex Biological Systems," *PLOS Comput. Biol.*, vol. 12, no. 5, p. e1004915, May 2016.

[8] M. K. Transtrum, B. B. Machta, and J. P. Sethna, "Geometry of nonlinear least squares with applications to sloppy models and optimization," *Phys. Rev. E*, vol. 83, no. 3, p. 036701, Mar. 2011.

[9] F. Bach, R. Jenatton, J. Mairal, and G. Obozinski, "Optimization with Sparsity-Inducing Penalties," *Found. Trends® Mach. Learn.*, vol. 4, no. 1, pp. 1–106, 2011.

[10] R. Jenatton, J.-Y. Audibert, and F. Bach, "Structured Variable Selection with Sparsity-Inducing Norms," *J. Mach. Learn. Res.*, vol. 12, no. Oct, pp. 2777–2824, 2011.

[11] Z. Ghahramani, "Probabilistic machine learning and artificial intelligence," *Nature*, vol. 521, no. 7553, pp. 452–459, May 2015.

[12] G. C. Kramer, R. A. Gunther, M. L. Nerlich, S. S. Zweifach, and R. H. Demling, "Effect of dextran-70 on increased microvascular fluid and protein flux after thermal injury.," *Circ. Shock*, vol. 9, no. 5, pp. 529–41, 1982.